

Microwave-assisted Synthesis of Green Inhibitor for Carbon Steel Acid Corrosion

Sami Ben Aoun * and Mouslim Messali

Department of Chemistry, Faculty of Science, Taibah University, PO. Box 30002 Al-Madinah Al-Munawarah, KSA.

*E-mail: sbenaoun@taibahu.edu.sa

Received: 27 December 2017 / Accepted: 10 February 2018 / Published: 6 March 2018

1-(3-bromopropyl)-4-(dimethylamino)pyridinium bromide (DPB) ionic liquid prepared via microwave-assisted synthesis was investigated as a potential corrosion inhibitor for carbon steel in molar hydrochloric acid solution by means of weight-loss method. The obtained results revealed the high inhibitive activity of the prepared ionic liquid with increasing inhibition efficiency reaching ca. 87.1% in the presence of 3×10^{-3} M DPB. The adsorptive nature of the inhibition process was proven by kinetics and thermodynamics investigations with a large adsorption constant ($K_{ads} = \text{ca. } 3.8 \times 10^3 \text{ mol}^{-1} \cdot \text{L}$) and an elevated activation energy ($E_a = \text{ca. } 83.1 \text{ kJ} \cdot \text{mol}^{-1}$). DPB was found to show a predominant physical adsorption onto the corroding carbon steel surface ($\Delta G_{ads} = \text{ca. } -35.9 \text{ kJ} \cdot \text{mol}^{-1}$). Electrochemical investigations revealed that DPB acted as a mixed-type corrosion inhibitor hindering both anodic and cathodic processes via blocking their respective active sites. The inhibitor was shown to form a protective layer resulting in increasing charge transfer resistance along with a decreasing double layer capacitance.

Keywords: Carbon steel; Corrosion; Ionic liquids; Gravimetric method; Langmuir isotherm; LPR; EIS.

1. INTRODUCTION

The widespread use of hydrochloric acid in a large variety of industries viz. descaling, pickling, acidizing and others [1-4] caused a worsening of the corrosion phenomena that affects almost every aspect of the industrialized world we currently live in. This spontaneous destruction of metal engineering structures, especially carbon steel which is by far the most employed material [5], has a tremendously bad impact on both human health and economy [6-8].

For decades now, scientists are concerned with the control and prevention of this unavoidable corrosion phenomenon through, among others, developing efficient corrosion inhibitors that were mainly organic compounds [9-16]. Of these, the ones having heteroatoms (i.e. N, S, O and P) and those

comprising π -electrons, especially aromatic rings, revealed the best inhibition efficiencies [17-30]. The driving force of this inhibitive activity lies in the strong adsorption of such compounds onto the dissolving metal. However, the use of most of these compounds results in several health problems and raises various environmental concerns [31].

A great deal of research focused on the preparation and use of more eco-friendly inhibitors [28, 32] and ionic liquids revealed to be a very interesting family of compounds, in this respect [27, 33-41], for instance for carbon steel corrosion [31, 33, 34, 42]. These compounds, as their names tell, are generally liquid at room temperature [43, 44], with great thermal stability, very low vapor pressure, superior conductivity and their ability to dissolve a large variety of compounds [45-48].

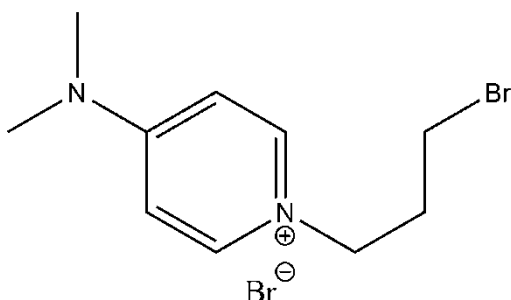
In this work, a microwave-assisted preparation of a pyridinium-based ionic liquid (DPB) was carried out, presenting the advantage of a green synthesis process leading to enhanced conversions and greatly reduced reaction times, and the prepared compound was applied for the corrosion inhibition of carbon steel in molar hydrochloric acid solution.

2. EXPERIMENTAL

2.1. Chemicals and materials:

Molar hydrochloric acid media was prepared by dilution with distilled water from a (37%) stock HCl solution (Panreac). All other chemicals used in this study were purchased from Sigma-Aldrich. Acetone (99.5%) and ethanol (99.8%) served for the cleaning of carbon steel specimen as described in the following section.

For the preparation of the investigated ionic liquid (cf. Scheme 1), the 4-dimethylaminopyridine nucleophilic alkylation with 1,3-dibromopropane in toluene was carried out under microwave irradiation (Discover SP microwave synthesizer, CEM Corp.) for 20 min at 100 °C. A mixture of 4-dimethylaminopyridine (1g, 8.2 mmol) and 1,3-dibromopropane (1.63g, 8.2 mmol) in 10 ml of toluene were placed in a closed container and exposed to microwave irradiation for 20 minutes at 100 °C. The precipitation of a solid from the initially obtained clear and homogenous mixture in toluene marked the completion of the reaction. The pyridinium-based ionic liquid was filtrated then washed thrice with ethyl acetate so that any unreacted starting materials and the solvent were removed. Finally, all volatile organic compounds were removed by drying the 1-(3-bromopropyl)-4-(dimethylamino)pyridinium bromide at a reduced pressure.



Scheme 1. Chemical structure of 1-(3-bromopropyl)-4-(dimethylamino)pyridinium bromide (DPB).

Adequate quantities of the inhibitor, which structure is given in Scheme 1, were dissolved in the as-prepared corrosive media in order to prepare the relevant concentrations of inhibitor.

A 0.5 mm-thick carbon steel sheet was mechanically polished then electrochemically cleaned before cutting into identical specimens and stored in a desiccator. Before every corrosion test measurements, each specimen was thoroughly cleaned with cleanser, acetone, and ethanol then thoroughly washed with distilled water, and dried.

2.2. Weight loss measurements:

For each experiment, a new as-prepared carbon steel specimen was precisely weighed by means of a GR-202 analytical balance (A&D Co. Ltd. Japan) then immersed for five hours in the corrosive media either in the presence or absence of (DPB). Afterwards, the specimen was taken out, cleaned with running tap water, acetone, ethanol then distilled water to ensure that no corrosion products are left on the metal surface. The dried specimen was then weighed again to determine the relevant weight loss.

2.3. Effect of Temperature:

The same experiments described above were repeated in thermostatic conditions utilizing an AI-controlled water bath (Yudian Co. Ltd., Hong Kong) at different working temperatures ranging between 296 and 343 K.

2.4. Electrochemical measurements:

A PGSTAT 128N autolab potentiostat/galvanostat (Metrohm, The Netherlands) was employed in all electrochemical experiments. Briefly, in linear polarization (LPR) experiments the potential scan was conducted in the window ± 100 mV vs. OCP (open circuit potential) with 1 mV.s^{-1} scan rate while in electrochemical impedance spectroscopy (EIS) a single sine wave perturbation of 10 mV amplitude was imposed under OCP conditions in a frequency range 0.1 MHz to 0.5 Hz. All potentials are reported versus SCE electrode.

3. RESULTS AND DISCUSSION

3.1. Characterization of DPB ionic liquid:

The desired ionic liquid was afforded easily in 81 % yield as solid. The results of various spectral analysis are shown in Figures 1-3.

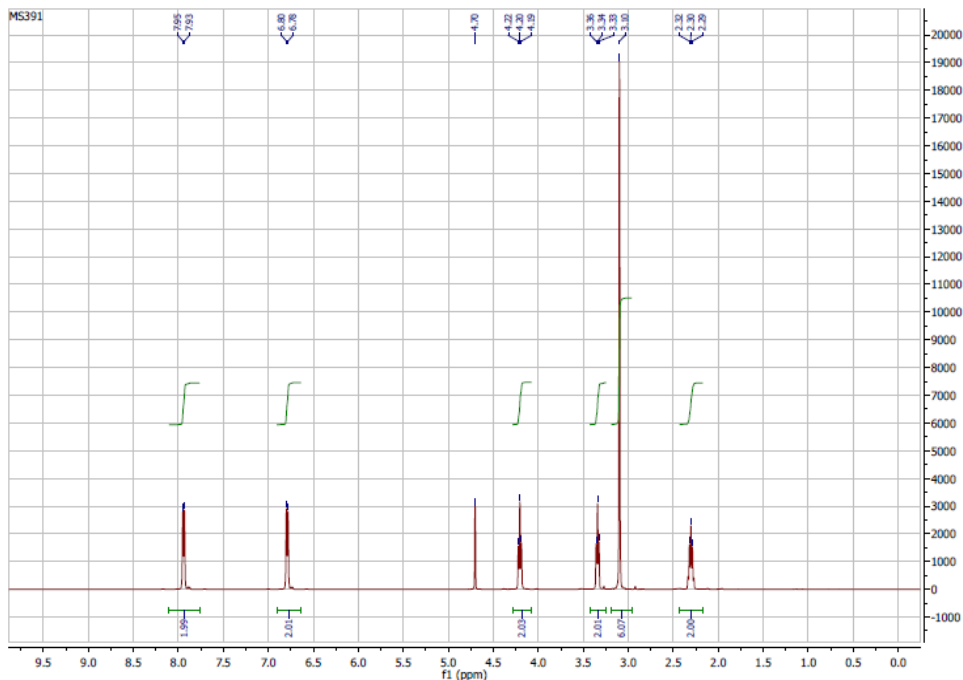


Figure 1. ^1H spectrum of 1-(3-bromopropyl)-4-(dimethylamino)pyridinium bromide.

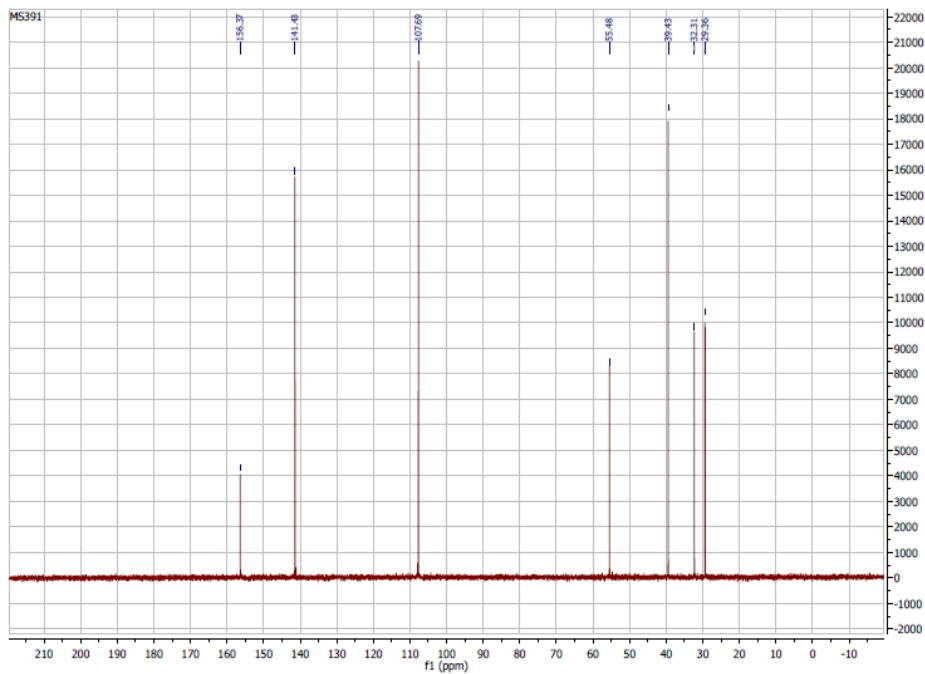


Figure 2. ^{13}C spectrum of 1-(3-bromopropyl)-4-(dimethylamino)pyridinium bromide.

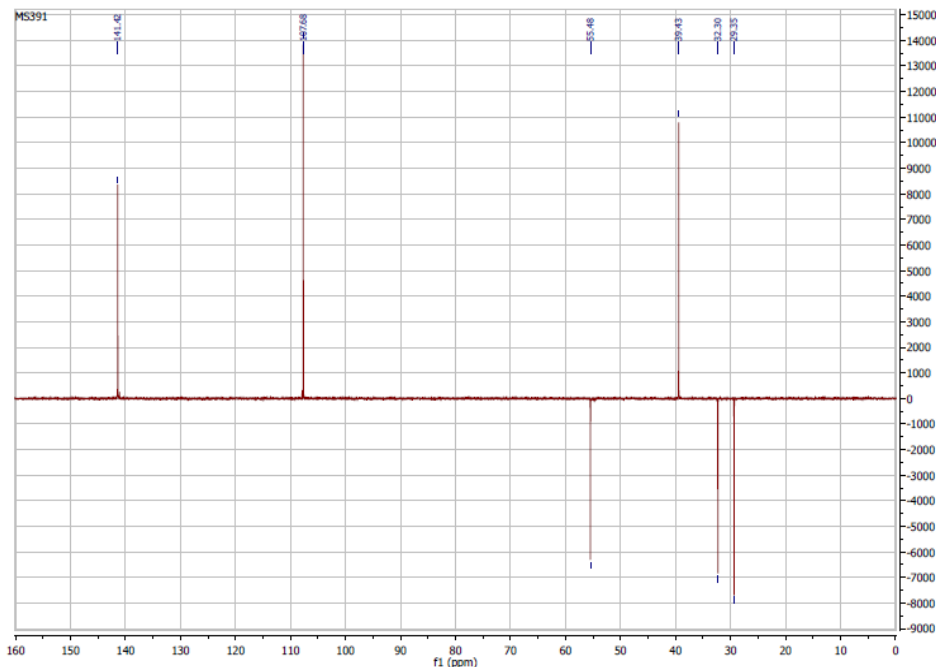


Figure 3. DEPT spectrum of 1-(3-bromopropyl)-4-(dimethylamino)pyridinium bromide.

^1H NMR (D_2O , 400 MHz); $\delta = 2.30$ (quintet, 2H), 3.10 (s, 6H), 3.34 (t, 2H), 4.20 (t, 2H), 6.78 (d, 2H), 7.93 (d, 2H); ^{13}C NMR (D_2O , 100 MHz); $\delta = 29.1$ (CH_2), 32.3 (CH_2), 39.4 (2CH_3), 55.5 (CH_2), 107.7 (CH), 141.4 (CH), 156.3 (C); IR (KBr) ν_{max} 3130 cm^{-1} (C-H Ar), $1596\text{-}1470 \text{ cm}^{-1}$ (C=C), 1164 cm^{-1} (C-N); LCMS (M-Br) 243.05 (97%) and 245.05 (100%) found for $\text{C}_{10}\text{H}_{16}\text{BrN}_2^+$.

3.2. Gravimetric study:

As expected, carbon steel was subjected to a very high corrosion when exposed to molar hydrochloric acid media shown as a high corrosion rate (CR) (i.e. ca. $0.185 \text{ mg.cm}^{-2}.\text{h}^{-1}$) evaluated by the equation:

$$CR = \frac{\Delta W}{At} \quad (1)$$

ΔW being the weight loss (mg), A the exposed surface area (15 cm^2 in this study) and t the exposure time (i.e. 5h).

The addition of $1\mu\text{M}$ of (DPB) to the corrosive media had a clear effect on the corrosion rate decreasing it to ca. $0.133 \text{ mg.cm}^{-2}.\text{h}^{-1}$ which shows the potential use of this compound as corrosion inhibitor, which efficiency (IE%) is determined as ca. 28.41% for this minute concentration, from the following equation:

$$IE\% = \left[\frac{CR^0 - CR^i}{CR^0} \right] \times 100 \quad (2)$$

Where CR^0 and CR^i are the corrosion rates in the absence and presence of inhibitor, respectively.

Increasing the DPB concentration promoted the inhibition efficiency and the results are displayed in Table 1. A very efficient corrosion inhibition (\approx ca. 87%) was obtained in the presence of 3 mM DPB ionic liquid, in the present work conditions.

Table 1. Gravimetric results for the corrosion parameters of carbon steel corrosion in 1 M HCl with various concentrations of DPB obtained at 296 K.

[DPB] (mol.L ⁻¹)	CR (mg.cm ⁻² .h ⁻¹)	IE %	θ
Blank	0.185	-----	-----
10⁻⁶	0.133	28.417	0.284
10⁻⁵	0.081	56.115	0.561
10⁻⁴	0.055	70.144	0.701
10⁻³	0.035	80.935	0.809
3×10⁻³	0.024	87.050	0.871

The data shown in Table 1 are presented in Figure 4 and Figure 5 as the effect on corrosion rate and inhibition efficiency, respectively, of DPB concentration. One can notice the sharp decrease in corrosion rate at the very beginning of DPB addition (cf. Figure 4) associated with a sharp increase in the inhibition efficiency (cf. Figure 5).

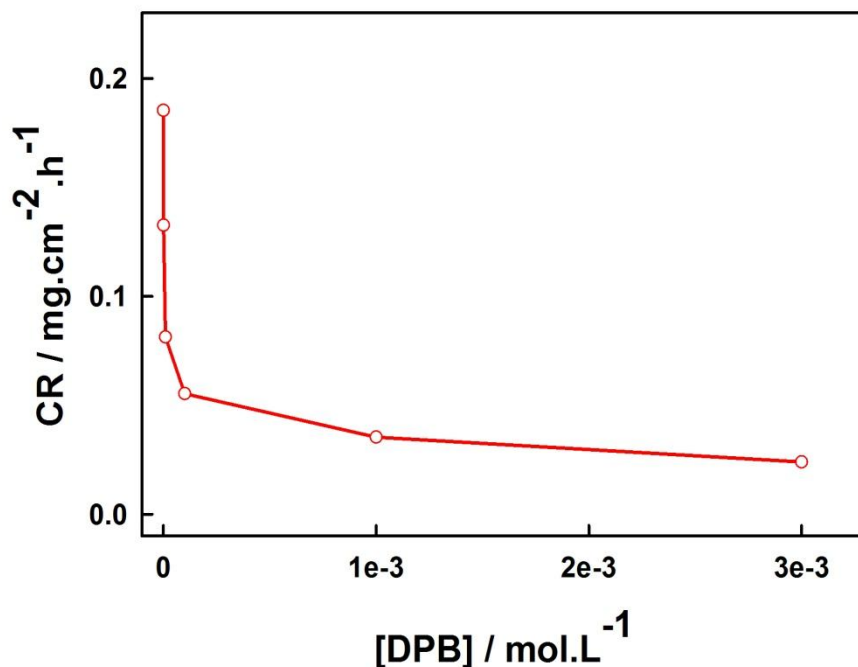


Figure 4. Effect on the corrosion rate (CR) of carbon steel of DPB concentration in 1 M HCl at 296 K.

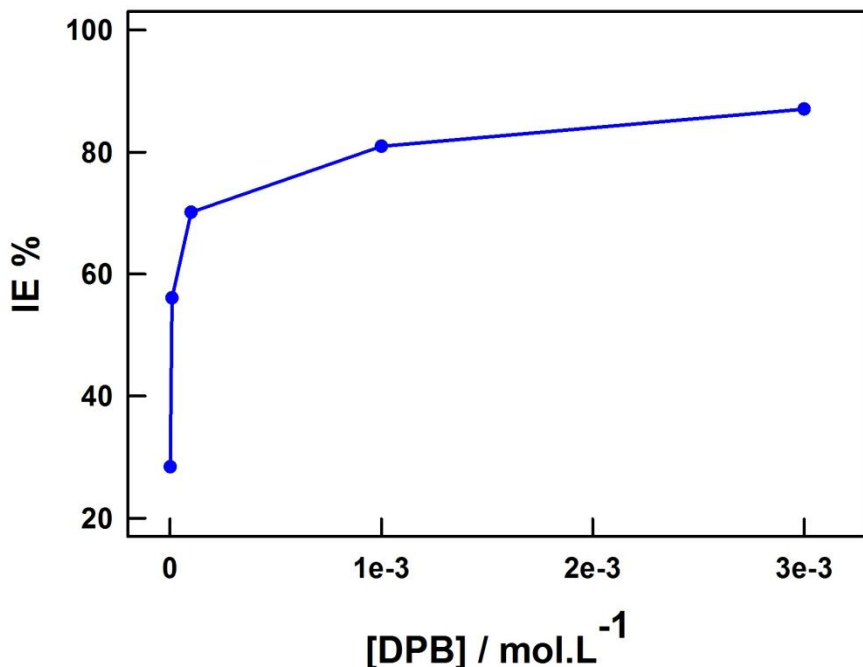


Figure 5. Effect on the inhibition efficiency (IE%) of carbon steel of DPB concentration in 1 M HCl at 296 K.

Such observation is explainable by the reduced exposed carbon steel surface to corrosive media in the presence of the DPB molecules as a result of their adsorption onto the metal surface, which eventually leads to replacement of adsorbed water molecules, blocking the corrosion active sites and hindering the acid attack on the metal surface [49-51]. This is confirmed by the increasing surface coverage (θ) of the carbon steel [34] as per the equation:

$$\theta = \frac{\text{IE}\%}{100} \quad (3)$$

3.3. Corrosion Kinetics:

Investigation of the corrosion kinetics in the presence of DPB ionic liquid was based on the equation:

$$\text{CR} = k[\text{DPB}]^a \quad (4)$$

k is the specific corrosion rate constant and a is the order of the corrosion process.

By taking the logarithm of both sides, the equation re-arranges as follows:

$$\log \text{CR} = \log k + a \log [\text{DPB}]$$

A plot of $\log \text{CR}$ against $\log [\text{DPB}]$, given in Figure 6, shows an excellent linearity ($R^2 = 0.991$) and the values of k and a were determined from the plot's intercept and slope, respectively. The obtained results are compiled in Table 2.

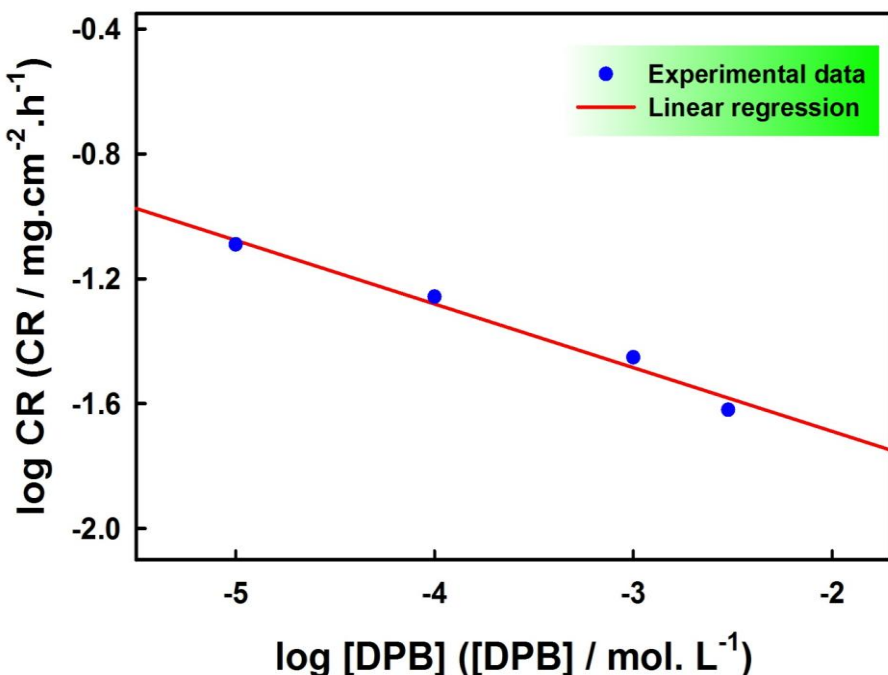


Figure 6. A plot of log CR vs. log [DPB] for carbon steel corrosion in 1 M HCl at 296 K.

Table 2. Kinetic parameters of carbon steel corrosion in 1 M HCl with various concentrations of DPB obtained at 296 K.

[DPB] (mol.L⁻¹)	0	10^{-6}	10^{-5}	10^{-4}	10^{-3}	3×10^{-3}
log [DPB]	-----	-6.000	-5.000	-4.000	-3.000	-2.523
CR (mg.cm⁻².h⁻¹)	0.185	0.133	0.081	0.055	0.035	0.024
Log CR	-0.732	-0.877	-1.090	-1.257	-1.452	-1.620
a				-0.204		
k (mg.cm⁻².h⁻¹) ^{1/n}					8.002×10^{-3}	

The investigated ionic liquid's inhibitive activity is proved by the negative sign of the order of the corrosion reaction in the presence of various concentrations of (DPB) and its relatively large value [31, 52].

3.4. Corrosion Thermodynamics:

An essential part in a corrosion study is the effect of temperature for it has a direct impact on the metal corrosion process. Yet, the nature of this effect is rather complex, particularly in acid media, due to the possible co-existence of several simultaneous processes leading to metal surface changes like rapid surface etching, inhibitor's desorption and sometimes its degradation [52, 53]. In addition, hydrogen reduction reaction would accompany the corrosion process and the evolved hydrogen

volume increases with increasing temperature resulting in increasing corrosion rate [33, 34] which goes in line with increasing energy required for the activated complex formation that yields the corrosion products [7, 54].

Table 3. Gravimetric results for the corrosion parameters of carbon steel corrosion in 1 M HCl in the absence and presence of 3×10^{-3} M DPB obtained at different working temperatures.

T (K)	CR ⁰ (mg.cm ⁻² .h ⁻¹)	CR ⁱ (mg.cm ⁻² .h ⁻¹)	IE %	θ
296	0.185	0.024	87.050	0.871
313	0.691	0.099	85.632	0.856
333	5.078	0.836	83.537	0.835
343	9.084	2.393	73.661	0.737

We carried on with 3 mM DPB-containing 1 M HCl solution and studied the temperature effect on both CR and IE% in the range 296-343K. The obtained data is shown in table 3. As expected, the CR increased, both in the absence and presence of 3 mM DPB, with ascending temperature with a noteworthy more pronounced increase in the latter situation (i.e. \approx two-fold). This trend is clearly shown in Figure 7.

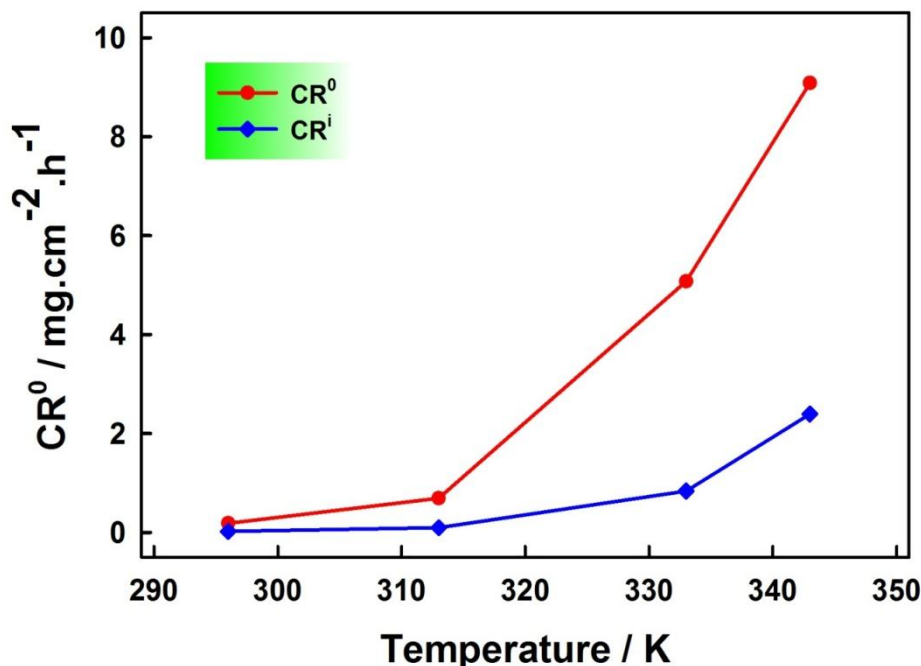


Figure 7. Temperature effect on the corrosion rate of carbon steel in 1 M HCl in the absence (CR⁰) and the presence (CRⁱ) of 3×10^{-3} M DPB.

As a consequence, a noticeable decrease of IE% is revealed from the examination of table 3 and that is shown in Figure 8. Such a behavior proves the adsorptive character of the DPB ionic liquid's inhibitive potential acting through blockage of the corrosion active sites onto the carbon steel surface [52, 55] as speculated in the previous section. In addition, this trend of IE% unveils the decreasing strength of DPB adsorption onto the corroding metal surface with increasing temperature [56] and perhaps their desorption, partially though, at elevated temperatures [57, 58]. Such remarks suggest a physical nature of the inhibitive molecules adsorption process (physisorption) in the present work conditions [59].

These assumptions are further proven by investigating the corrosion process's activation energy (E_a) change accompanying the addition of DPB into the corrosive media. For this, an Arrhenius-like temperature (T) dependence of the corrosion rate (CR) is mathematically represented by [7]:

$$CR = A \exp \left[-\frac{E_a}{RT} \right] \quad (5)$$

A being the pre-exponential factor and R the universal gas constant.

Plotting $\ln CR$ against $(1/T)$ using the data in Table 3 shows a linear relationship both in the absence ($R^2 = 0.993$) and presence ($R^2 = 0.991$) of DPB as displayed in Figure 9.

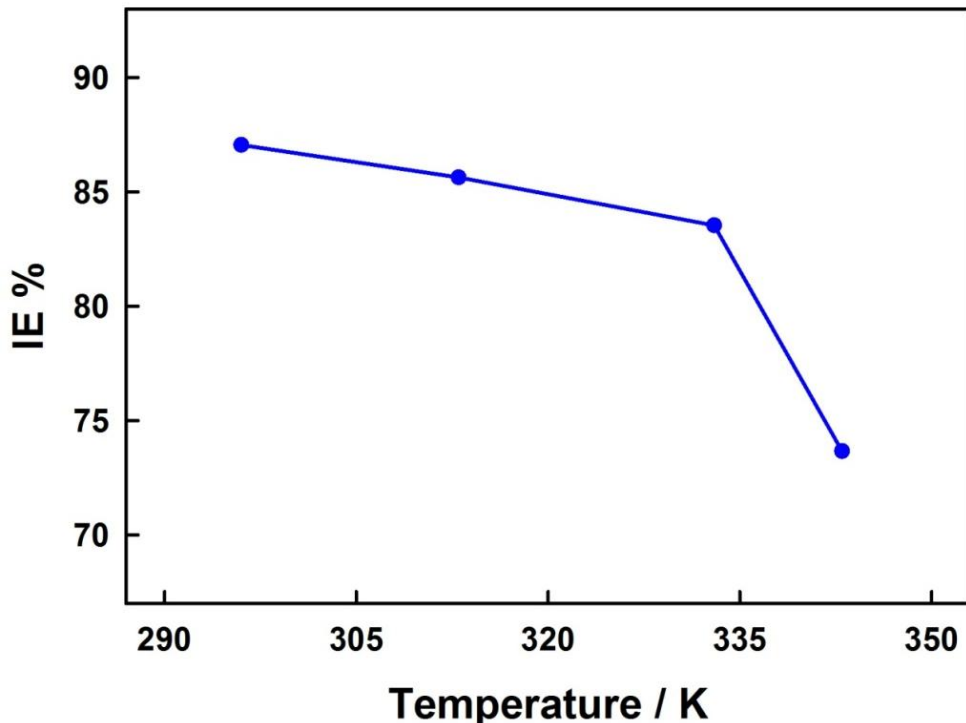


Figure 8. Temperature effect on the inhibition efficiency (IE%) of carbon steel corrosion in a $(3 \times 10^{-3}$ M DPB + 1 M HCl) solution.

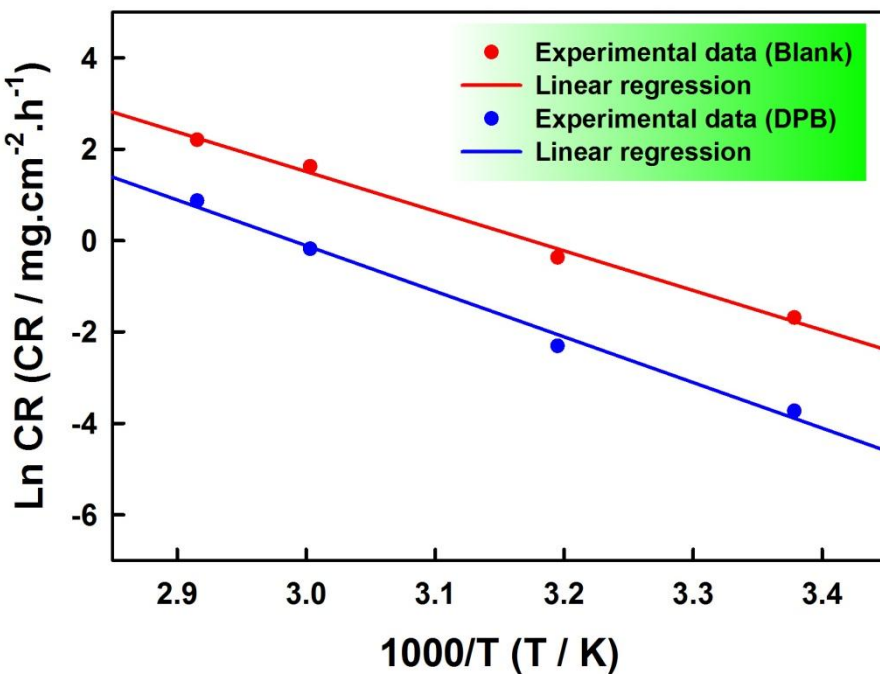


Figure 9. Arrhenius plots for carbon steel corrosion rates (CR) in 1 M HCl in the presence and absence of 3×10^{-3} M DPB.

In each case, the slope (i.e. $-E_a/R$) and the intercept (i.e. $\ln A$) permit the determination of the Arrhenius parameters (i.e. A and E_a) and these are shown in Table 4.

Table 4. Corrosion thermodynamic parameters for carbon steel in 1 M HCl with and without 3×10^{-3} M DPB.

Solution	Fig.9 slope	Fig.9. intercept	Fig.10 slope	Fig.10. intercept	A ($\text{mg.cm}^{-2}.\text{h}^{-1}$)	E_a kJ.mol^{-1}	ΔH_a kJ.mol^{-1}	ΔS_a J.mol^{-1}
Blank	-8.680	27.551	-8.362	20.787	9.229×10^{11}	72.169	69.523	-24.723
DPB	-9.999	29.889	-9.680	23.124	9.560×10^{12}	83.134	80.488	-5.284

The observed increase in activation energy in the presence of 3 mM DPB (i.e. $\approx 11 \text{ kJ/mol}$) is indicative of an elevation of the corrosion process's energy barrier [57] which confirms the strong adsorption of DPB molecules onto the corroding carbon steel surface resulting in the formation of a thicker double layer at the metal-corrosive media interface [58]. It also favors the physical nature of the adsorption process of DPB molecules onto the corroding metal surface [52]. In both cases, $E_a > 20 \text{ kJ.mol}^{-1}$, which confirms the existence of a surface-reaction process [59]. Moreover, the ten-fold increase of the pre-exponential factor (cf. Table 4) observed in the presence of DPB is an additional confirmation of its superior inhibiting potential [33].

Considering the transition-state formulation of Arrhenius equation, where N and h are, respectively, Avogadro's and Plank's constants:

$$CR = \frac{RT}{Nh} \exp\left(\frac{\Delta S_a}{R}\right) \exp\left(-\frac{\Delta H_a}{RT}\right) \quad (6)$$

and by plotting $\ln(CR/T)$ against $(1/T)$ as displayed in Figure 10, we were able to evaluate additional thermodynamic parameters viz. the activation enthalpy (ΔH_a) and activation entropy (ΔS_a) in both inhibited and uninhibited corrosion processes (cf. Table 4).

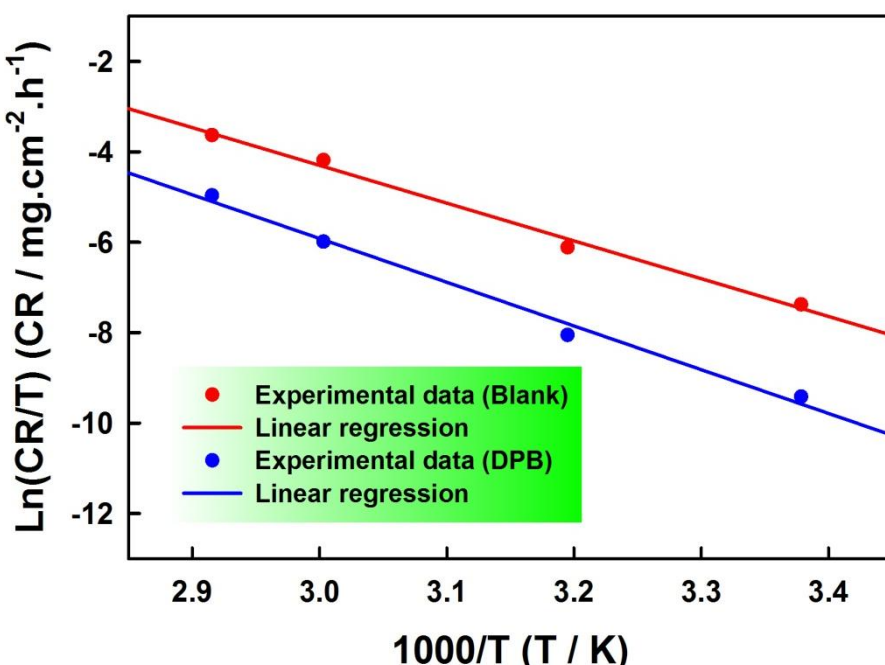


Figure 10. Transition-state plots for carbon steel corrosion rates (CR) in 1 M HCl in the presence and absence of 3×10^{-3} M DPB.

Inspection of Table 4 shows that the activation energy, whether in the absence or presence of DPB, has higher values compared with the activation enthalpy as a consequence of the hydrogen evolution reaction inducing a decrease of the volume [31, 33, 34].

In addition, the difference between these two parameters retained a constant value in both situations (i.e. ca. 2.65 kJ/mol) and is almost identical to the average value of (RT) , that is ca. 2.67 kJ/mol in this case, which indicates a unimolecular corrosion process [50].

As for the activation entropy, the noticeable increase in the presence of DPB ionic liquid confirms the water molecules replacement due to inhibitor's adsorption onto carbon steel surface [31] while its negative sign reveals that the rate-determining step involves an association-based activated complex formation [60]. The observation that ΔS_a bears a negative sign either in the absence or presence of inhibitor is well reported in literature [61-64].

3.5. Adsorption Isotherm:

The inhibition mechanism of the investigated DPB ionic liquid is intrinsically related to its adsorption which is presented as an adsorption isotherm [7, 57, 58, 65]. The common ones are Temkin, Frumkin, Flory-Huggins, Freundlich and Langmuir isotherms [7, 57, 58, 66]. The latter is shown to be

the one to which the obtained results fit the best (i.e. $R^2 = 0.999$). In this case, a Langmuirian isotherm is described by the following relationship between the adsorption constant (K_{ads}), the surface coverage (θ) and the inhibitor concentration (C^{inh}):

$$\frac{C^{inh}}{\theta} = \frac{1}{K_{ads}} + C^{inh} \quad (7)$$

which is plotted in Figure 11 as (C^{inh} / θ) vs. (C^{inh}) , the slope of which yields the value of (K_{ads}) and the results are summarized in Table 5. The large value of this constant (i.e. ca. 3.834×10^3) agrees well with the large inhibition efficiency obtained in the current study explainable here by the quite strongly adsorbed ionic liquid molecules onto the corroding metal surface.

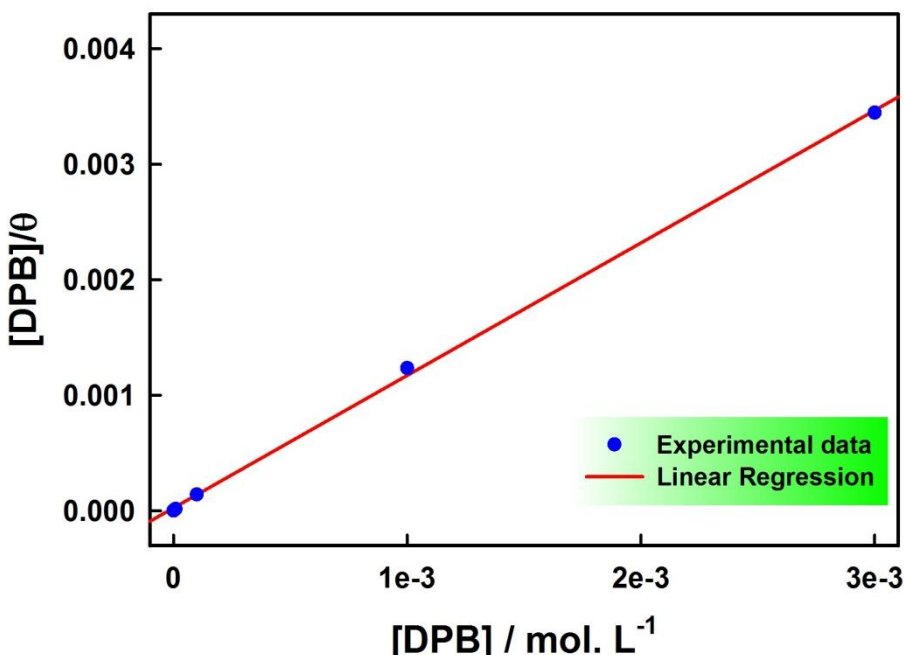


Figure 11. Langmuir adsorption isotherm of DPB on carbon steel surface in 1 M HCl at 296 K.

Table 5. Thermodynamic parameters for the adsorption of DPB onto the carbon steel surface in 1 M HCl.

Inhibitor	Slope	K_{ads} (mol⁻¹.L)	R^2	ΔG_{ads} (kJ.mol⁻¹)
DPB	1.147	3.834×10^3	0.999	-35.860

Since the DPB adsorption follows a Langmuir isotherm, we can conclude the absence of intermolecular forces between the adsorbed inhibitor's molecules [67].

A very important thermodynamic parameter is the adsorption free energy (ΔG_{ads}) which can be determined from the equation:

$$\Delta G_{\text{ads}} = -RT \ln (K_{\text{ads}} \times C_{\text{solvent}}) \quad (8)$$

using the value of 55.5 mol/L for the concentration of water and the previously determined value of the adsorption constant, the adsorption free energy (ΔG_{ads}) was evaluated to ca. -35.860 kJ/mol (cf. Table 5). Since the adsorption free energy bears a negative sign, this indicates the spontaneity of DPB molecules adsorption onto the carbon steel surface.

The classification of the type of adsorption relates to the magnitude of its free energy, for instance $|\Delta G_{\text{ads}}| \leq 20 \text{ kJ/mol}$ are commonly regarded as physical adsorption while $|\Delta G_{\text{ads}}| \geq 40 \text{ kJ/mol}$ is an indication of chemical adsorption [7, 31, 33, 34, 62, 68]. Looking at the currently obtained results, the involved adsorption would be mixed-type in nature [69, 70] with a predominant physisorption [33, 71]. The adsorption mechanism on DPB molecules onto the corroding carbon steel surface is therefore believed to be mainly driven by electrostatic forces in addition to a contributing sharing and/or transfer of electrons between the metal surface and the inhibitor involving, most probably, both cathodic and anodic sites [33, 50]. This chemisorption contribution is expected as a result of the existing lone pairs on both nitrogen and bromine (cf. Scheme 1) in addition to the π -system of the aromatic ring driving the adsorption to higher strength, rather than a pure physisorption, and leading to high inhibition efficiencies [72, 73].

3.6. Electrochemical study:

LPR voltammograms in the absence and presence of various DPB concentrations are displayed in Fig. 12 showing Tafel lines for both cathodic and anodic branches in all cases revealing the activation-controlled nature of the related reactions [42, 58, 74].

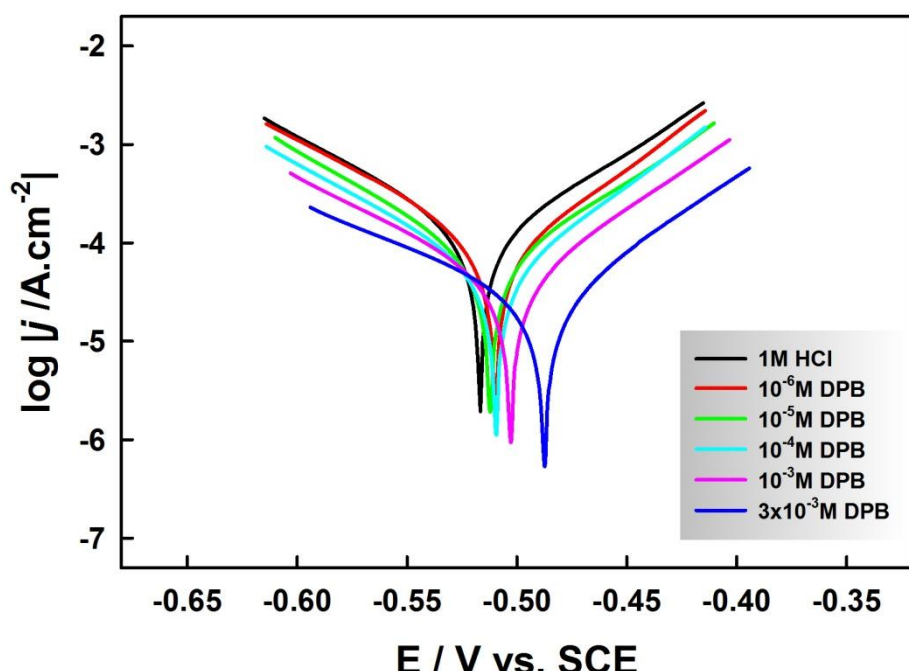


Figure 11. Carbon steel linear polarization curves in 1 M HCl with different concentrations of DPB.

In addition, it can be noted that none of these reactions mechanism (i.e. metal dissolution and hydrogen evolution) was altered in the presence of DPB inhibitor as revealed by the similar general shape of the voltammograms [68].

The extracted corrosion parameters are collected in Table 6. Namely, the corrosion potential (E_{corr}), the corrosion current (I_{corr}), the anodic and cathodic Tafel constants (b_a and b_c). It was then possible to calculate the inhibition efficiency (IE%) and surface coverage (θ) from the following equations:

$$IE\% = \frac{I_{corr}^0 - I_{corr}}{I_{corr}^0} \times 100 \quad (9)$$

$$\theta = 1 - \frac{I_{corr}}{I_{corr}^0} \quad (10)$$

I_{corr}^0 and I_{corr} being the corrosion currents in the absence and presence of inhibitor, respectively.

Table 6 Polarization results for the corrosion parameters of carbon steel corrosion in 1 M HCl with various concentrations of (DPB) obtained at 296 K.

[DPB] (mol.L ⁻¹)	E_{corr} (mV)	I_{corr} (A.cm ⁻²)	b_a (mV.dec ⁻¹)	b_c (mV.dec ⁻¹)	IE %	θ
Blank	-517	1.51E-04	94	92
10⁻⁶	-514	1.14E-04	92	91	24.5	0.245
10⁻⁵	-512	7.94E-05	87	86	47.6	0.476
10⁻⁴	-510	5.72E-05	73	87	62.2	0.622
10⁻³	-503	4.44E-05	73	96	70.7	0.707
3×10⁻³	-488	2.77E-05	71	119	81.7	0.817

The negligibly varying slopes, especially for the metal dissolution reaction, as shown in Table 6 confirm the blocking of respective active sites [31, 42] and the decreasing current densities upon DPB additions to the corrosive media which is observed on both branches indicates the inhibition efficiency of DPB molecules acting on both cathodic and anodic processes, with a slightly more effect on the latter [31, 42].

The IE% increased monotonously with increasing inhibitor concentration reaching ca. 82% in the presence of 3 mM DPB ionic liquid in a very good agreement with the weight loss results. This is likely due to increasingly adsorbed DPB molecules onto the corroding carbon steel [62]. This is supported by the increasing surface coverage (θ) as shown in table 6. On the other hand, the slightly changed corrosion potential (≤ 85 mV) shows that DPB acts as a mixed-type corrosion inhibitor in the present work conditions [31, 42].

This electrochemical investigation is further complemented by EIS which results are shown as Niquist plots in Fig. 12 exhibiting a single capacitive loop which again confirms that the corrosion process remains activation-controlled [66] both in the absence and presence of DPB as revealed by LPR data. And here also, the similar shapes of the plots with various inhibitor concentrations confirm the non-alteration of the corrosion reaction mechanism upon addition of DPB molecules [57].

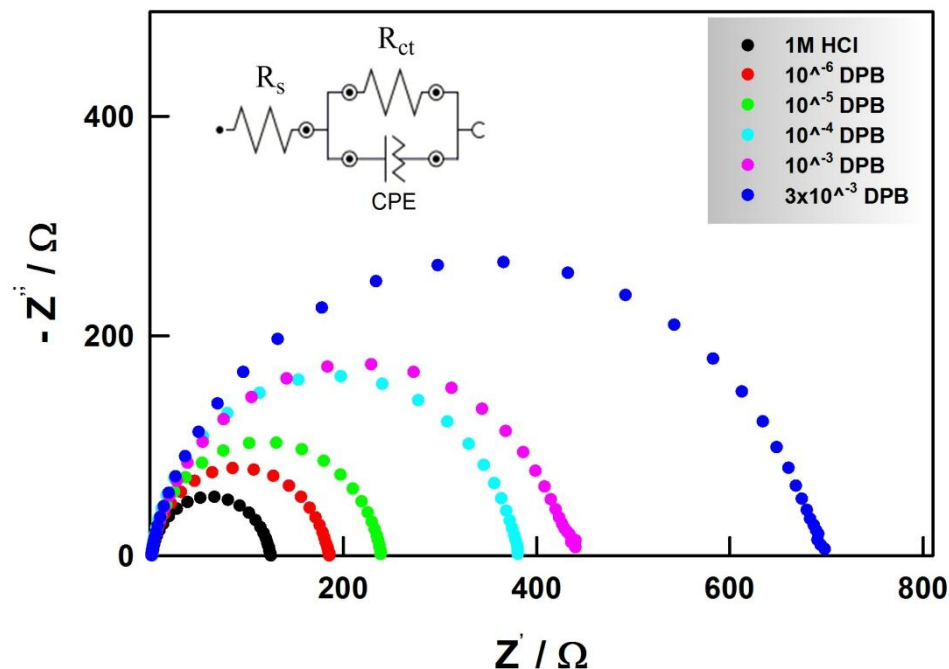


Figure 12. Carbon steel Nyquist plots in 1 M HCl with different concentrations of DPB.

The experimental data was fitted to the equivalent circuit shown in the inset of Fig. 12 where R_s and R_{ct} represent the solution resistance and charge transfer resistance, respectively. The latter being inversely proportional the corrosion rate and its value, relative to the one in the absence of inhibitor (i.e. R_{ct}^0), is an indication of the inhibition efficiency as per the equation:

$$\text{IE\%} = \frac{R_{ct}^0 - R_{ct}}{R_{ct}^0} \times 100 \quad (11)$$

while the surface coverage (θ) can be calculated using the equation:

$$\theta = \frac{R_{ct}^0 - R_{ct}}{R_{ct}^0} \quad (12)$$

It is noteworthy that the double layer impedance fitting is realized by the introduction of a constant phase element (CPE, of Y_0 value and n exponent) into the equivalent electrical circuit instead of a pure capacitance since the observed capacitive loops differ from perfect circular shapes [31, 42] and the impedance (Z_{CPE}) in this case is given, considering that $j=\sqrt{-1}$, by the equation:

$$Z_{CPE} = \frac{1}{Y_0(jw)^n} \quad (13)$$

The double layer capacitance (C_{dl}) values can then be calculated from the equation [66, 68]:

$$C_{dl} = \sqrt[n]{Y_0 R_{ct}^{1-n}} \quad (14)$$

And all the extracted parameters are given in Table 7.

Table 7 Electrochemical impedance spectroscopy parameters for the corrosion parameters of carbon steel corrosion in 1 M HCl with various concentrations of (DPB) obtained at 296 K.

[DPB] (mol.L ⁻¹)	R ⁰ _{ct} (Ω.cm ²)	R _{ct} (Ω.cm ²)	IE%	θ	Y ₀ (Mho.cm ⁻²)	n	C _{dl} (F.cm ⁻²)
Blank	122.7	122.7	5.72E-05	0.916	3.63E-05
10⁻⁶	122.7	183.9	33.3	0.333	5.87E-05	0.914	3.84E-05
10⁻⁵	122.7	237.0	48.2	0.482	4.91E-05	0.914	3.23E-05
10⁻⁴	122.7	376.5	67.4	0.674	4.13E-05	0.921	2.88E-05
10⁻³	122.7	430.1	71.5	0.715	4.15E-05	0.880	2.40E-05
3×10⁻³	122.7	679.1	81.9	0.819	3.34E-05	0.873	1.93E-05

The clearly noticed increasing diameters of the capacitive loops in Fig. 12 due to the increasing charge transfer resistance as depicted in Table 7 confirms the effective inhibiting activity of DPB and that is indicative of the formation of a protective layer onto the corroding metal-corrosive media interface [57, 62, 66] leading to increasing IE% values reaching ca. 82% in a very good agreement with LPR data. This layer's formation and growth is confirmed by increasing surface coverage values reaching up to ca. 0.82 as shown in Table 7. This is further supported by the clearly decreasing double layer capacitance values as a consequence of the replacement of the adsorbed water molecules by DPB molecules [57, 58, 68] as per the relationship:

$$C_{dl} = \frac{\epsilon_0 \times \epsilon_r}{\delta} \quad (15)$$

showing that the double layer capacitance is inversely proportional to the thickness of the protective film (δ).

4. CONCLUSION

The inhibitive activity of DPB for carbon steel corrosion in 1M HCl was investigated in the present study. Weigh loss measurements revealed a clear inhibitory activity in the presence of as less as 1 μ M DPB which increased with increasing concentration and reached ~ca. 90% at 3 mM concentration. Such observation is explainable by the reduced exposed carbon steel surface to corrosive media in the presence of the DPB molecules as a result of their adsorption onto the metal surface, which eventually leads to replacement of adsorbed water molecules, blocking the corrosion active sites and hindering the acid attack on the metal surface. From kinetics study, the inhibitive activity of the investigated ionic liquid was proved by the negative sign of the order of the corrosion reaction in the presence of various concentrations of (DPB) and its relatively large value. While thermodynamics investigations showed a noticeable decrease of IE% with increasing temperature suggesting a physical nature of the inhibitive molecules adsorption process (physisorption) in the present work conditions. This was further supported by the observed increase in activation energy in the presence of 3 mM DPB and clearly confirmed by the value of ($\Delta G_{ads} = -35.860$ kJ/mol) proving that a predominantly physisorption is behind the observed corrosion inhibition.

Further electrochemical investigations were in an excellent agreement with the weight loss results. For instance LPR data revealed the excellent inhibiting activity of DPB which blocks, at the same time, the metal dissolution and the hydrogen reduction active sites and therefore reduced both anodic and cathodic current densities. The investigated ionic liquid was also shown to be a mixed-type corrosion inhibitor. Moreover, EIS experiments confirmed this conclusion and showed that the inhibitor's adsorption onto the corroding metal surface resulted in the formation of a protective layer leading to a great increase of charge transfer resistance against a pronounced decrease of the double layer capacitance.

ACKNOWLEDGEMENT

The authors acknowledge the financial support received from the Deanship of Scientific Research, Taibah University through the research Grant No. 6257/1435.

References

1. D. Ben Hmamou, M.R. Aouad, R. Salghi, A. Zarrouk, M. Assouag, O. Benali, M. Messali, H. Zarrok, B. Hammouti, *J. Chem. Pharm. Res.*, 4 (2012) 3489-3497.
2. A.H. Al Hamzi, H. Zarrok, A. Zarrouk, R. Salghi, B. Hammouti, S.S. Al-Deyab, M. Bouachrine, A. Amine, F. Guenoun, *Intern. J. Electrochem. Sci.*, 8 (2013) 2586-2605.
3. C. Crowe, J. Masmonteil, R. Thomas, *Oilfield Rev.*, 4 (1992) 22.
4. R. Solmaz, *Corros. Sci.*, 81 (2014) 75-84.
5. S. Ben Aoun, M. Bouklah, K.F. Khaled, B. Hammouti, *Intern. J. Electrochem. Sci.*, 11 (2016) 7343-7358.
6. V.S. Saji, *Recent Patents on Corrosion Science*, 2 (2010) 6-12.
7. M.R. Laamari, J. Benzakour, F. Berrekhis, A. Derja, D. Villemin, *Arab. J. Chem.*, 9, Supplement 1 (2016) S245-S251.
8. S. Kharchouf, L. Majidi, M. Bouklah, B. Hammouti, A. Bouyanzer, A. Aouniti, *Arab. J. Chem.*, 7 (2014) 680-686.
9. M. Yadav, D. Sharma, S. Kumar, *Korean J. Chem. Eng.*, 32 (2015) 993-1000.

10. S.A.S. Dias, S.V. Lamaka, C.A. Nogueira, T.C. Diamantino, M.G.S. Ferreira, *Corros. Sci.*, 62 (2012) 153-162.
11. M. Yu, M. Liang, J. Liu, S. Li, B. Xue, H. Zhao, *Appl. Surf. Sci.*, 363 (2016) 229-239.
12. S. Peng, W. Zhao, H. Li, Z. Zeng, Q. Xue, X. Wu, *Appl. Surf. Sci.*, 276 (2013) 284-290.
13. E. Roussi, A. Tsetsekou, A. Skarmoutsou, C.A. Charitidis, A. Karantonis, *Surf. Coat. Technol.*, 232 (2013) 131-141.
14. I. Santana, A. Pepe, E. Jimenez-Pique, S. Pellice, I. Milošev, S. Ceré, *Surf. Coat. Technol.*, 265 (2015) 106-116.
15. A.C. Balaskas, I.A. Kartsonakis, D. Snihirova, M.F. Montemor, G. Kordas, *Progress in Organic Coatings*, 72 (2011) 653-662.
16. S. Zheng, J. Li, *J. Sol-Gel Sci. Technol.*, 54 (2010) 174-187.
17. M. Dahmani, A. Et-Touhami, S.S. Al-Deyab, B. Hammouti, A. Bouyanzer, *Intern. J. Electrochem. Sci.*, 5 (2010) 1060-1069.
18. A.Y. Musa, A.A.H. Kadhum, A.B. Mohamad, M.S. Takriff, A.R. Daud, S.K. Kamarudin, *Corros. Sci.*, 52 (2010) 526-533.
19. E.M. Sherif, S.M. Park, *Electrochim. Acta*, 51 (2006) 1313-1321.
20. E.M. Sherif, S.M. Park, *J. Electrochem. Soc.*, 152 (2005) B428-B433.
21. K.R. Ansari, Sudheer, A. Singh, M.A. Quraishi, *J. Dispersion Sci. Technol.*, 36 (2015) 908-917.
22. N. Caliskan, E. Akbas, *Mater. Chem. Phys.*, 126 (2011) 983-988.
23. X. Li, X. Xie, S. Deng, G. Du, *Corros. Sci.*, 87 (2014) 27-39.
24. L. Bai, L.-J. Feng, H.-Y. Wang, Y.-B. Lu, X.-W. Lei, F.-L. Bai, *RSC Advances*, 5 (2015) 4716-4726.
25. A.O. Yüce, G. Kardaş, *Corros. Sci.*, 58 (2012) 86-94.
26. M.A. Chidiebere, E.E. Oguzie, L. Liu, Y. Li, F. Wang, *Mater. Chem. Phys.*, 156 (2015) 95-104.
27. M. Finşgar, D. Kek Merl, *Corros. Sci.*, 83 (2014) 164-175.
28. S. Hari Kumar, S. Karthikeyan, *J. Mater. Environ. Sci.*, 4 (2013) 675-684.
29. M. Yadav, S. Kumar, U. Sharma, P.N. Yadav, *J. Mater. Environ. Sci.*, 4 (2013) 691-700.
30. K.R. Ansari, M.A. Quraishi, A. Singh, *Measurement*, 76 (2015) 136-147.
31. S. Ben Aoun, *RSC Advances*, 7 (2017) 36688-36696.
32. B. Zhang, C. He, C. Wang, P. Sun, F. Li, Y. Lin, *Corros. Sci.*, 94 (2015) 6-20.
33. S. Ben Aoun, *Der Pharma Chemica*, 5 (2013) 294-304.
34. S. Ben Aoun, *Intern. J. Electrochem. Sci.*, 8 (2013) 10788-10804.
35. X. Zhou, H. Yang, F. Wang, *Electrochim. Acta*, 56 (2011) 4268-4275.
36. P. Huang, J.-A. Latham, D.R. MacFarlane, P.C. Howlett, M. Forsyth, *Electrochim. Acta*, 110 (2013) 501-510.
37. N.V. Likhanova, M.A. Domínguez-Aguilar, O. Olivares-Xometl, N. Nava-Entzana, E. Arce, H. Dorantes, *Corros. Sci.*, 52 (2010) 2088-2097.
38. I. Lozano, E. Mazario, C.O. Olivares-Xometl, N.V. Likhanova, P. Herrasti, *Mater. Chem. Phys.*, 147 (2014) 191-197.
39. Q. Zhang, Y. Hua, *Mater. Chem. Phys.*, 119 (2010) 57-64.
40. X. Zheng, S. Zhang, W. Li, M. Gong, L. Yin, *Corros. Sci.*, 95 (2015) 168-179.
41. M. Scendo, J. Uznanska, *International Journal of Corrosion*, 2011 (2011).
42. S. Ben Aoun, *Intern. J. Electrochem. Sci.*, 12 (2017) 10369-10380.
43. N. Jain, A. Kumar, S. Chauhan, S.M.S. Chauhan, *Tetrahedron*, 61 (2005) 1015-1060.
44. J.S. Wilkes, *Green Chemistry*, 4 (2002) 73-80.
45. H.L. Ngo, K. LeCompte, L. Hargens, A.B. McEwen, *Thermochim. Acta*, 357-358 (2000) 97-102.
46. P. Bonhte, A.P. Dias, N. Papageorgiou, K. Kalyanasundaram, M. Grätzel, *Inorg. Chem.*, 35 (1996) 1168-1178.
47. S.A. Forsyth, J.M. Pringle, D.R. MacFarlane, *Australian Journal of Chemistry*, 57 (2004) 113-119.
48. F. Endres, S. Zein El Abedin, *Phys. Chem. Chem. Phys.*, 8 (2006) 2101-2116.

49. F. Bentiss, M. Traisnel, M. Lagrenée, *Corros. Sci.*, 42 (2000) 127-146.
50. L. Larabi, O. Benali, Y. Harek, *Mater. Lett.*, 61 (2007) 3287-3291.
51. L. Larabi, Y. Harek, O. Benali, S. Ghalem, *Progress in Organic Coatings*, 54 (2005) 256-262.
52. E.A. Noor, *Intern. J. Electrochem. Sci.*, 2 (2007) 996-1017.
53. F.Z. Bouanis, F. Bentiss, M. Traisnel, C. Jama, *Electrochim. Acta*, 54 (2009) 2371-2378.
54. N.A. Negm, A.M.A. Sabagh, M.A. Migahed, H.M.A. Bary, H.M.E. Din, *Corros. Sci.*, 52 (2010) 2122-2132.
55. I. El Ouali, B. Hammouti, A. Aouniti, Y. Ramli, M. Azougagh, E.M. Essassi, M. Bouachrine, *J. Mater. Environ. Sci.*, 1 (2010) 1-8.
56. L. Afia, N. Rezki, M.R. Aouad, A. Zarrouk, H. Zarrok, R. Salghi, B. Hammouti, M. Messali, S.S. Al-Deyab, *Intern. J. Electrochem. Sci.*, 8 (2013) 4346-4360.
57. J. Haque, K.R. Ansari, V. Srivastava, M.A. Quraishi, I.B. Obot, *Journal of Industrial and Engineering Chemistry*, 49 (2017) 176-188.
58. K.R. Ansari, M.A. Quraishi, A. Singh, S. Ramkumar, I.B. Obote, *RSC Advances*, 6 (2016) 24130-24141.
59. A. Zarrouk, H. Zarrok, R. Salghi, B. Hammouti, F. Bentiss, R. Touir, M. Bouachrine, *J. Mater. Environ. Sci.*, 4 (2013) 177-192.
60. S.S. Abd El Rehim, H.H. Hassan, M.A. Amin, *Mater. Chem. Phys.*, 70 (2001) 64-72.
61. E.A. Noor, *Corros. Sci.*, 47 (2005) 33-55.
62. M.R. Laamari, J. Benzakour, F. Berrekhis, M. Bakasse, D. Villemin, *Arab. J. Chem.*, 9, Supplement 2 (2016) S1218-S1224.
63. M.A.M. Ibrahim, M. Messali, Z. Moussa, A.Y. Alzahrani, S.N. Alamry, B. Hammouti, *Portug. Electrochim. Acta*, 29 (2011) 375-389.
64. D. Ben Hmamou, R. Salghi, A. Zarrouk, M. Messali, H. Zarrok, M. Errami, B. Hammouti, L. Bazzi, A. Chakir, *Der Pharma Chemica*, 4 (2012) 1496-1505.
65. D. Ben Hmamou, M.R. Aouad, R. Salghi, A. Zarrouk, M. Assouag, O. Benali, M. Messali, H. Zarrok, B. Hammouti, *J. Chem. Pharm. Res.*, 4 (2012) 3498-3504.
66. H. Lgaz, R. Salghi, S. Jodeh, B. Hammouti, *J. Mol. Liq.*, 225 (2017) 271-280.
67. V.V. Torres, V.A. Rayol, M. Magalhães, G.M. Viana, L.C.S. Aguiar, S.P. Machado, H. Orofino, E. D'Elia, *Corros. Sci.*, 79 (2014) 108-118.
68. R. Laamari, J. Benzakour, F. Berrekhis, A. Abouelfida, A. Derja, D. Villemin, *Arab. J. Chem.*, 4 (2011) 271-277.
69. A. Ghazoui, N. Benchaft, S.S. Al-Deyab, A. Zarrouk, B. Hammouti, M. Ramdani, M. Guenbour, *Intern. J. Electrochem. Sci.*, 8 (2013) 2272-2292.
70. A. Anejjar, A. Zarrouk, R. Salghi, D. Ben Hmamou, H. Zarrok, S.S. Al-Deyab, M. Bouachrine, B. Hammouti, N. Benchat, *Intern. J. Electrochem. Sci.*, 8 (2013) 5961-5979.
71. A. Guendouz, N. Missoum, A. Chetouani, S.S. Al-Deyab, B. Ben Cheikhe, N. Boussalah, B. Hammouti, M. Taleb, A. Aouniti, *Intern. J. Electrochem. Sci.*, 8 (2013) 4305-4327.
72. C. Verma, M.A. Quraishi, A. Singh, *J. Mol. Liq.*, 212 (2015) 804-812.
73. C.B. Verma, E.E. Ebenso, I. Bahadur, I.B. Obot, M.A. Quraishi, *J. Mol. Liq.*, 212 (2015) 209-218.
74. S. Issaadi, T. Douadi, A. Zouaoui, S. Chafaa, M.A. Khan, G. Bouet, *Corros. Sci.*, 53 (2011) 1484-1488